

Probing Nanoscale Damage Gradients in Irradiated Metals using Nano-mechanical Test Techniques

Siddhartha (Sid) Pathak

Assistant Professor

Department of Materials Science and Engineering

Iowa State University

pathak@iastate.edu

Acknowledgement:

Dr. Manish Jain, Soumya Varma, Cayla Harvey, Skye Supakul, Anugraha TK,
Deeksha Kodangal, Manish Kumar (UNR, ISU)

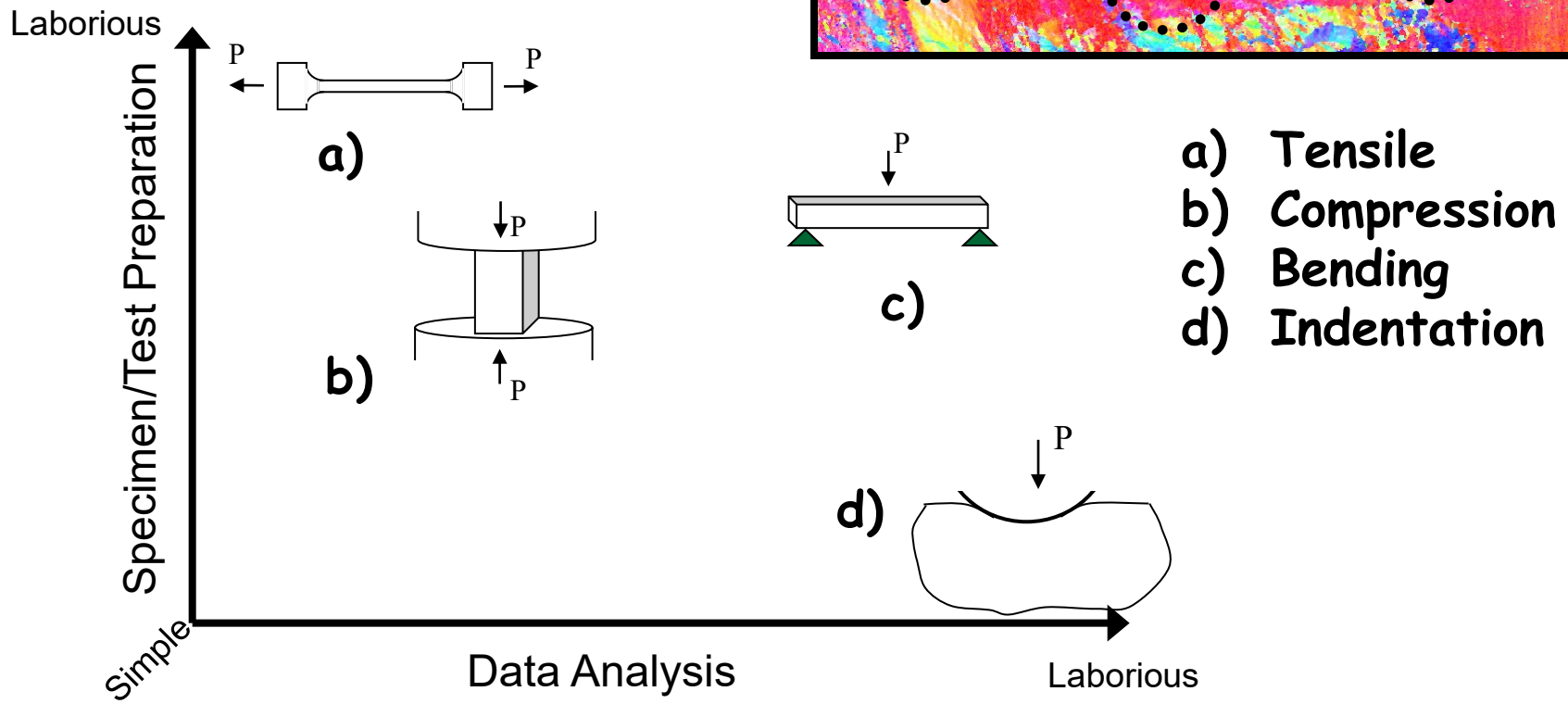
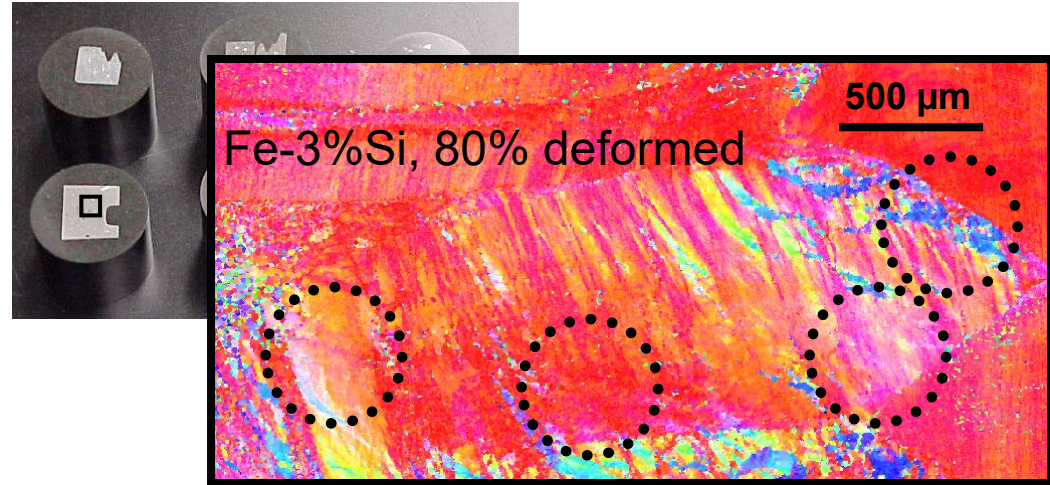
NSF, DOE, NASA, AFOSR, ARO, DARPA

DURIP, NSF MRI, DOE NEUP Scientific Infrastructure Support

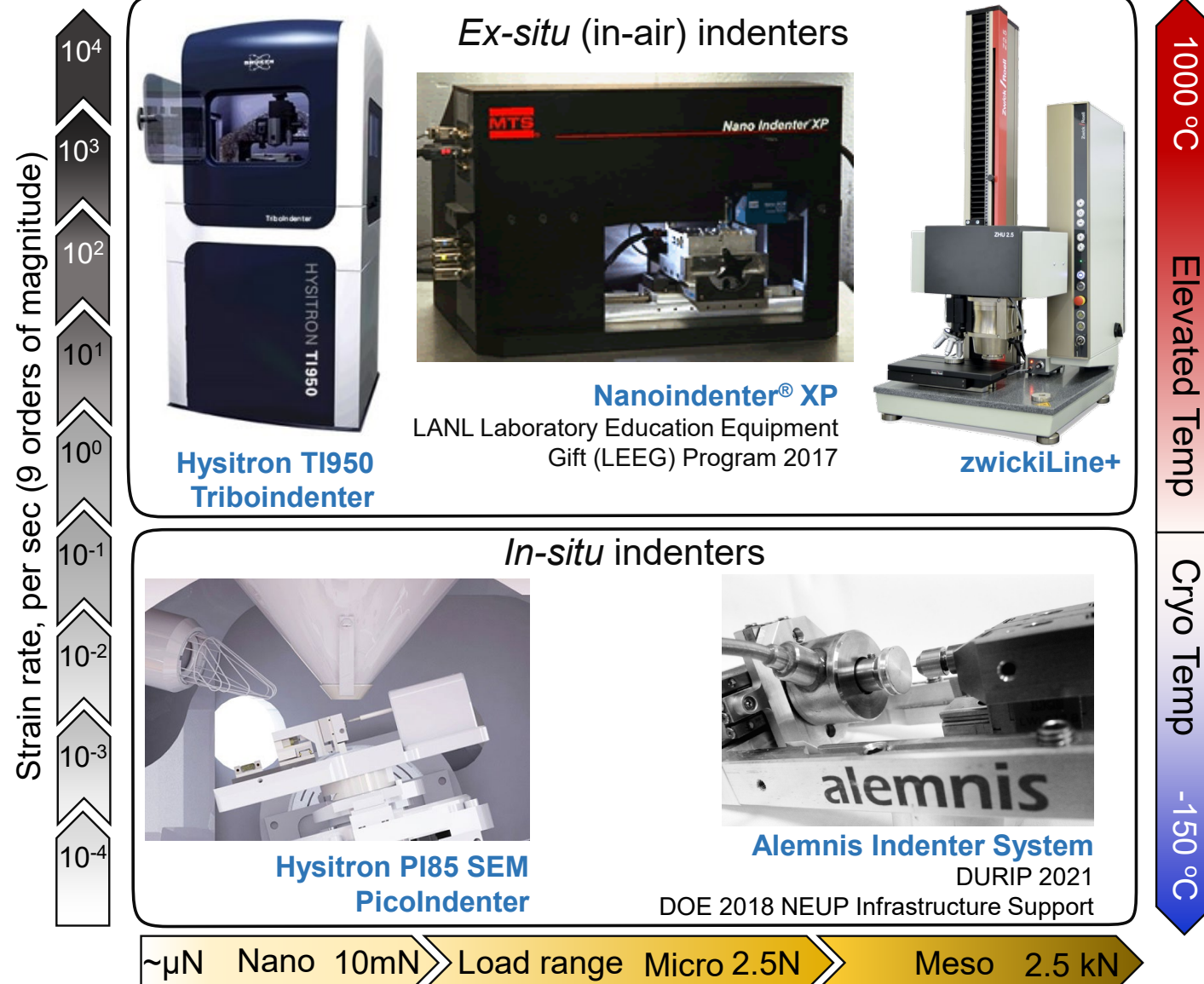
Mechanical Testing Tools at the Micro-scale

Crystal Plasticity models at the micron (grain) scale:
missing information

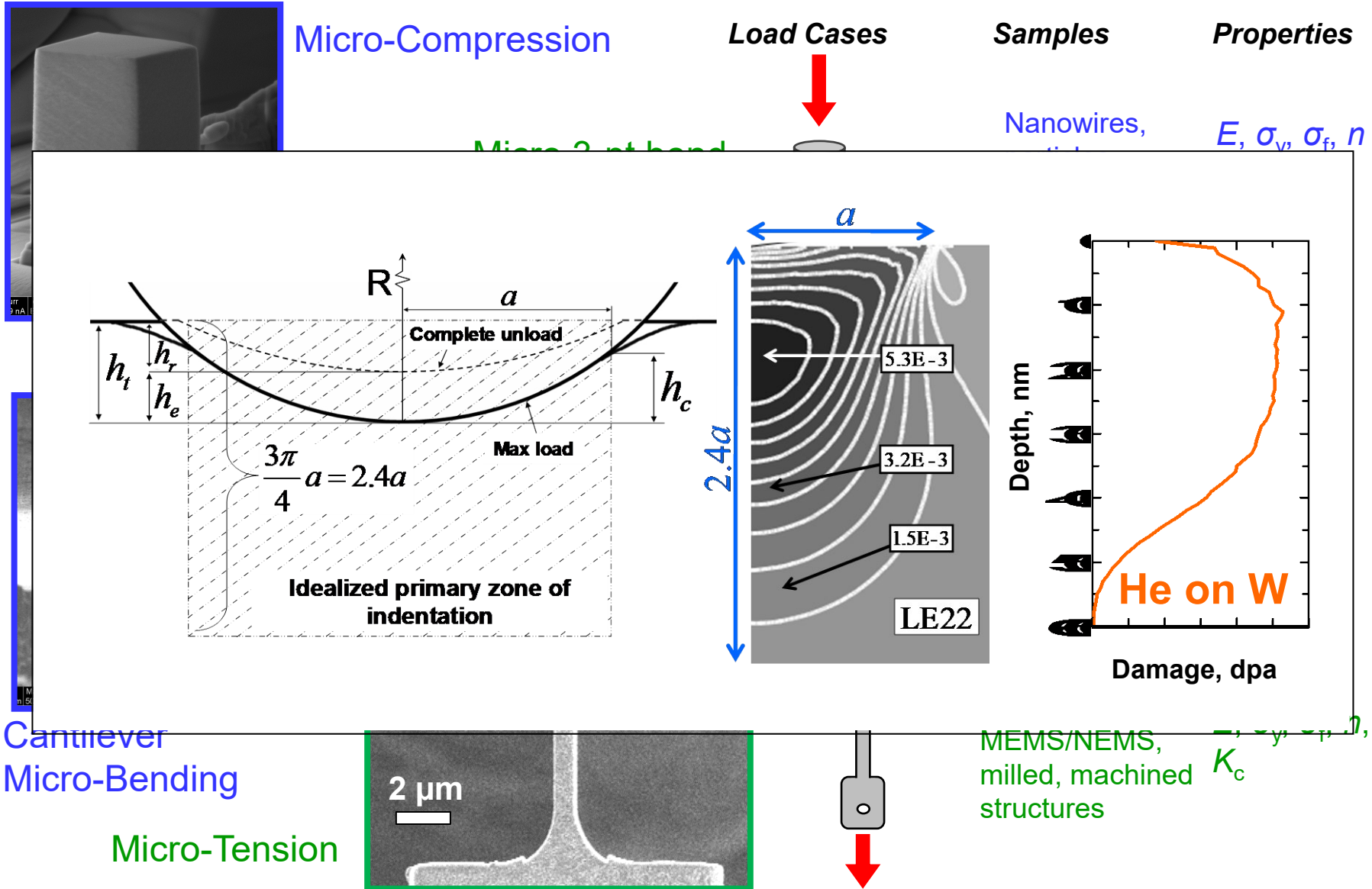
– grain scale heterogeneity of dislocation density,
both between grains and within the same grain



Investigating local mechanical response at the micro- and nano-scales: Capabilities under extreme conditions



Investigating local mechanical response at the micro- and nano-scales: *In-situ* SEM straining capabilities



Outline

- Extraction of Spherical Nanoindentation Stress Strain curves
- Indentation on anisotropic samples
 - Characterizing the anisotropy in indentation modulus
 - Characterizing the local indentation yield strength
- Probing nanoscale damage gradients with spherical nanoindentation
- Comparing small scale mechanical test techniques for measuring irradiation hardening

Spherical Nanoindentation Basics

Hertz Principle

$$h_e = \left(\frac{3P}{4E_{eff}} \right)^{\frac{2}{3}} \left(\frac{1}{R_{eff}} \right)^{\frac{1}{3}}$$

$$\frac{1}{E_{eff}} = \left(\frac{1-v^2}{E} \right)_{sample} + \left(\frac{1-v^2}{E} \right)_{indenter}$$

$$\frac{1}{R_{eff}} = \frac{1}{R_i} + \frac{1}{R_s} \quad a = fn(R_{eff})$$

E_{eff} = Effective Modulus

E_i = Modulus of Indenter

E_s = Modulus of Sample

v_i = Poisson Ratio of Indenter

v_s = Poisson Ratio of Sample

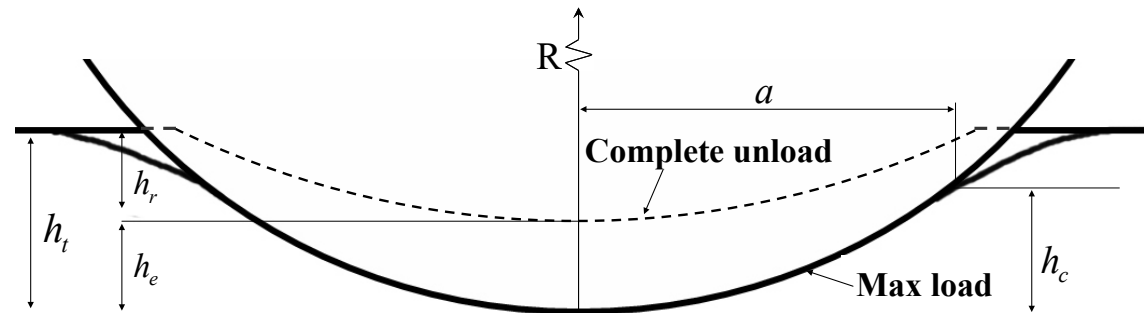
R_{eff} = Effective indentation radius

R_i = Radius of curvature of the indenter tip

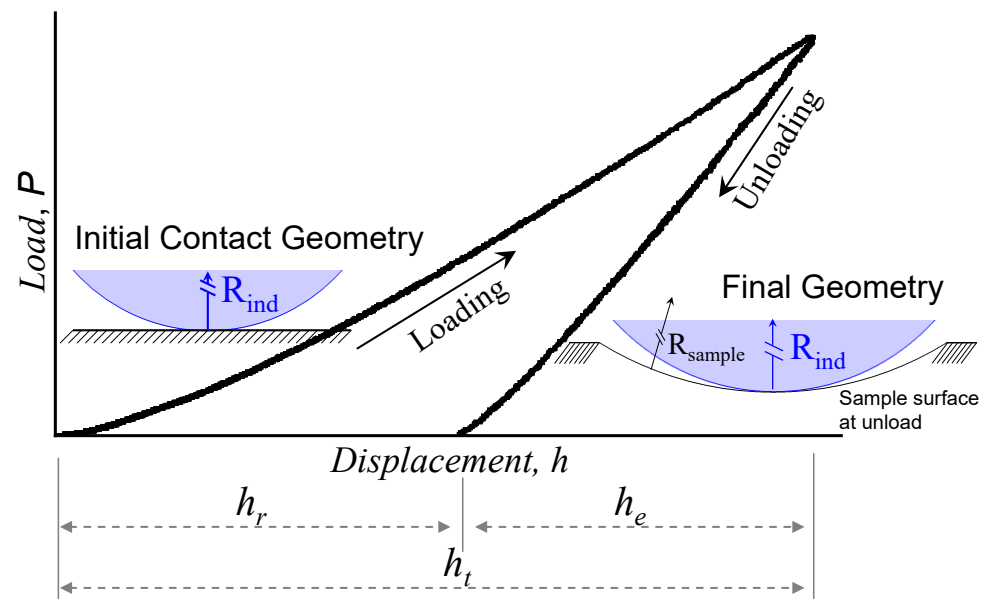
P = Load

h_e = elastic depth

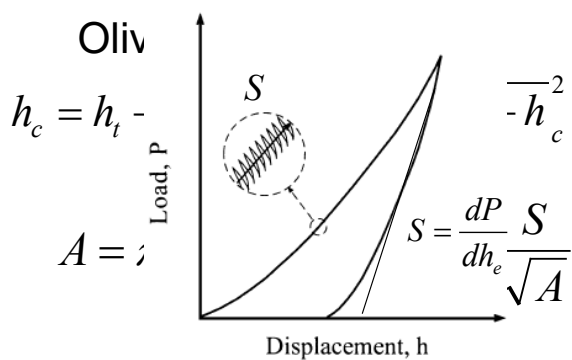
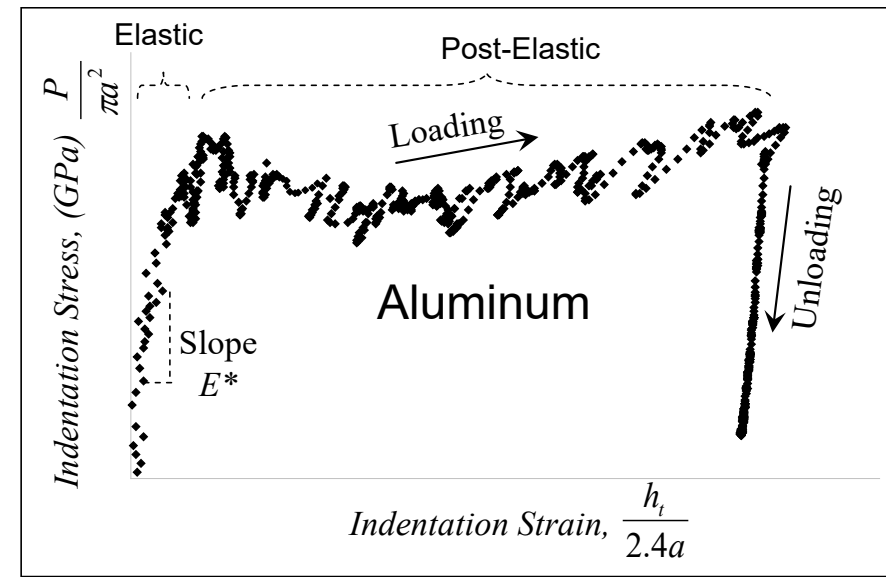
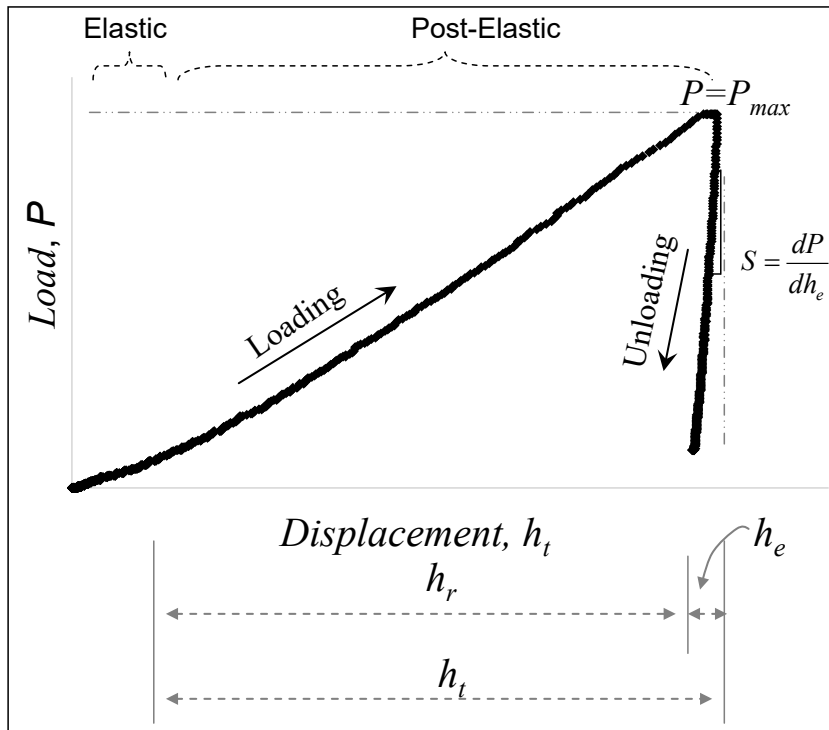
a = contact radius



Assumptions: linear elastic, isotropic material response, frictionless contact



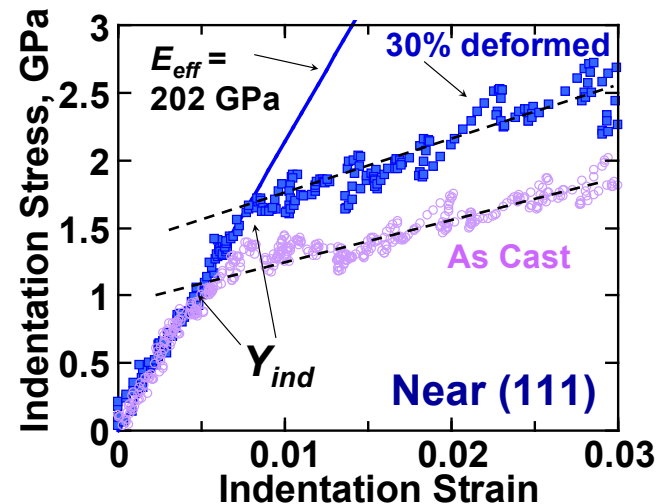
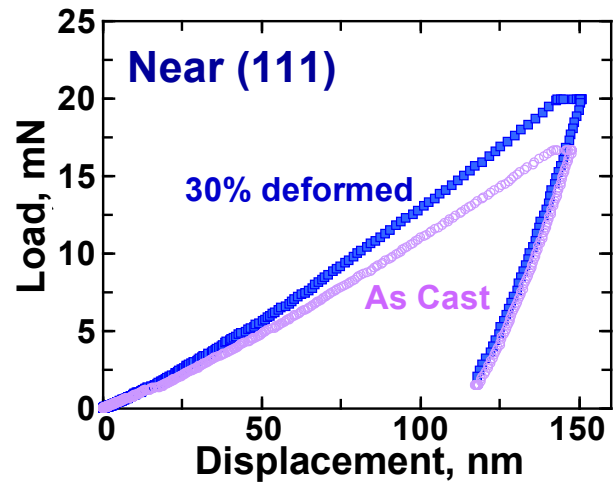
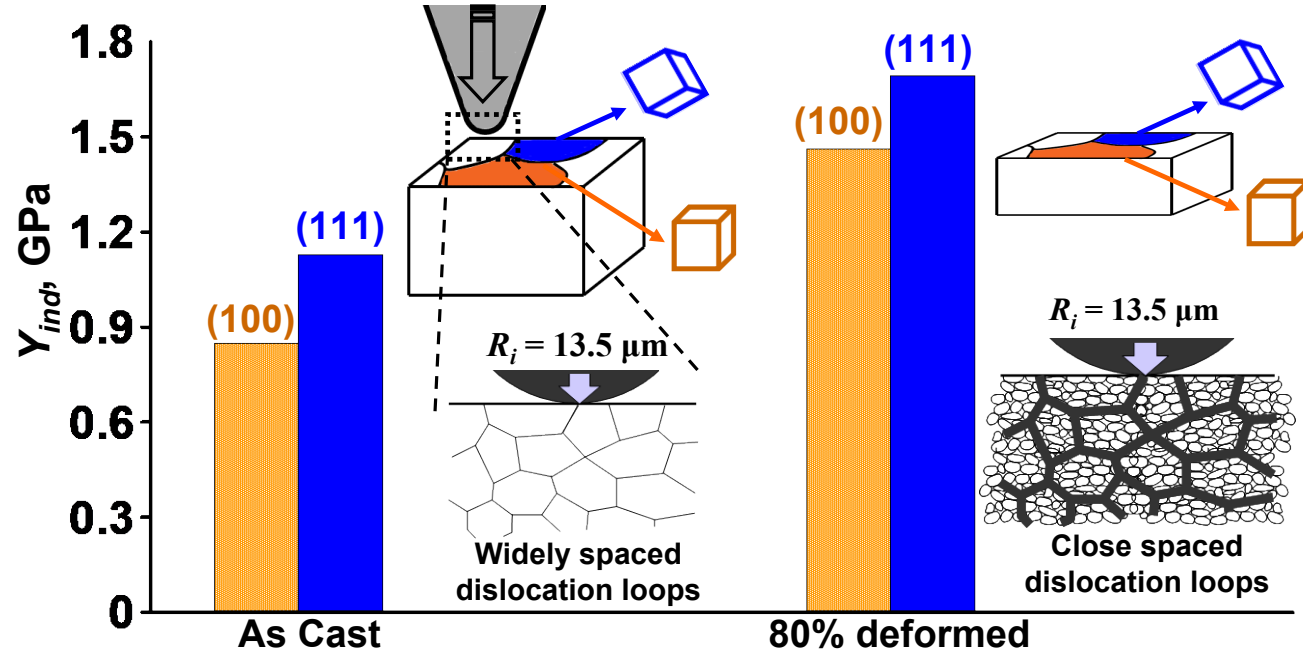
Generating Nanoindentation Stress and Strain Curves



- determine an effective zero point
- calculate E_{eff} from the initial elastic loading segment where $R_{eff} = R_i$
- estimate the contact radius
- $\sigma_{ind} = E_{eff} \epsilon_{ind}$

$$\sigma_{ind} = \frac{P}{\pi a^2} \quad \epsilon_{ind} = \frac{4}{3\pi} \frac{h_t}{a}$$

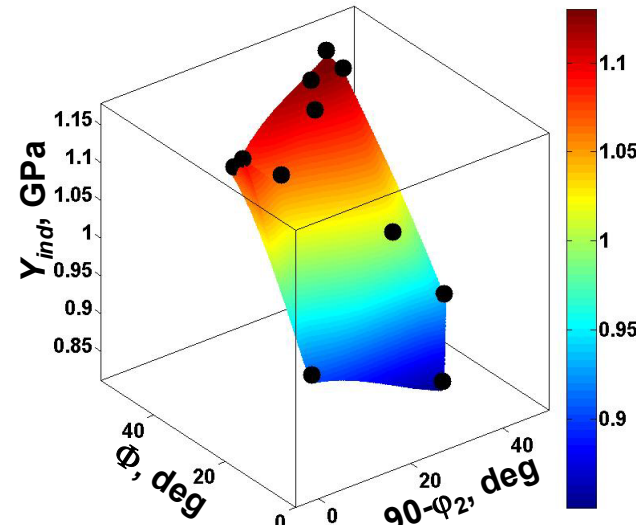
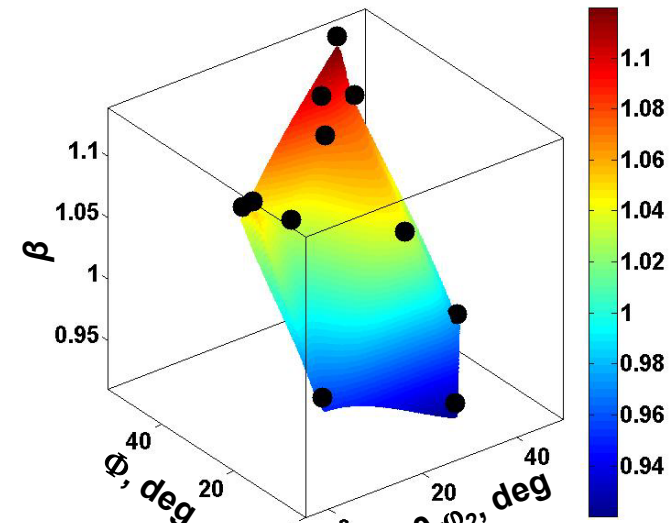
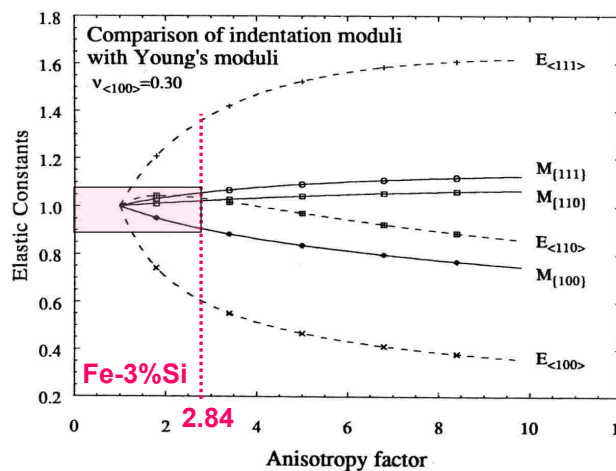
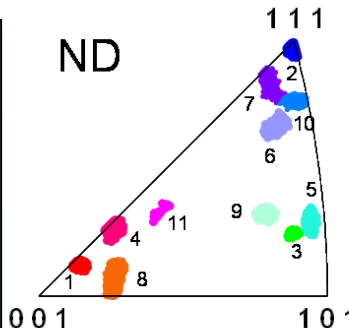
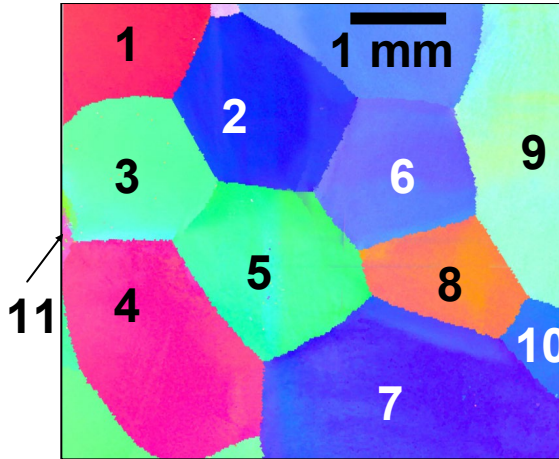
Nanoindentation on anisotropic samples



Hertz theory for anisotropic samples, Yield Surface Maps

$$\frac{1}{E_{eff}} = \frac{1}{\beta} \left(\frac{1 - \nu_s^2}{E_s} \right)_{isotropic} + \left(\frac{1 - \nu_i^2}{E_i} \right)_{indenter}$$

Fe-3%Si As cast

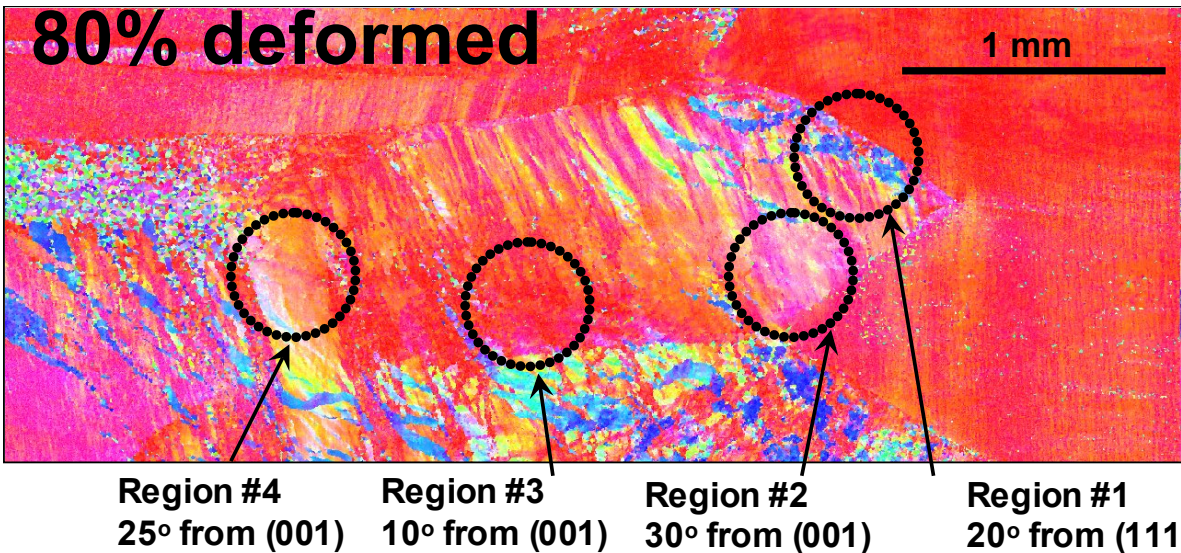
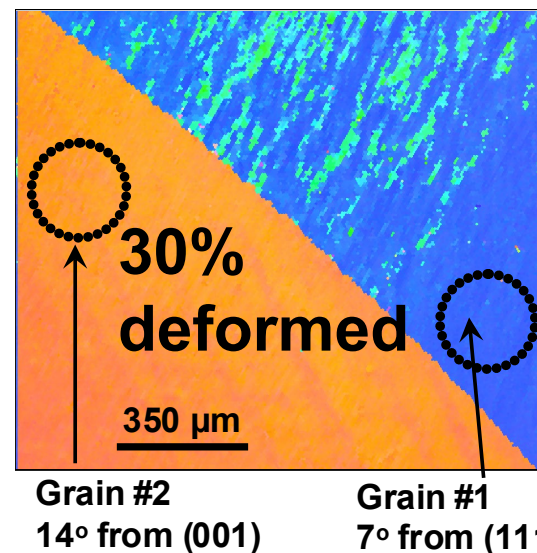


Estimating $\Delta\tau_{CRSS}$ for deformed samples

$$Y_{ind} = M(\Phi, \varphi_2) \tau_{CRSS}$$

$$\Delta\tau_{CRSS} \propto \sqrt{\rho}$$

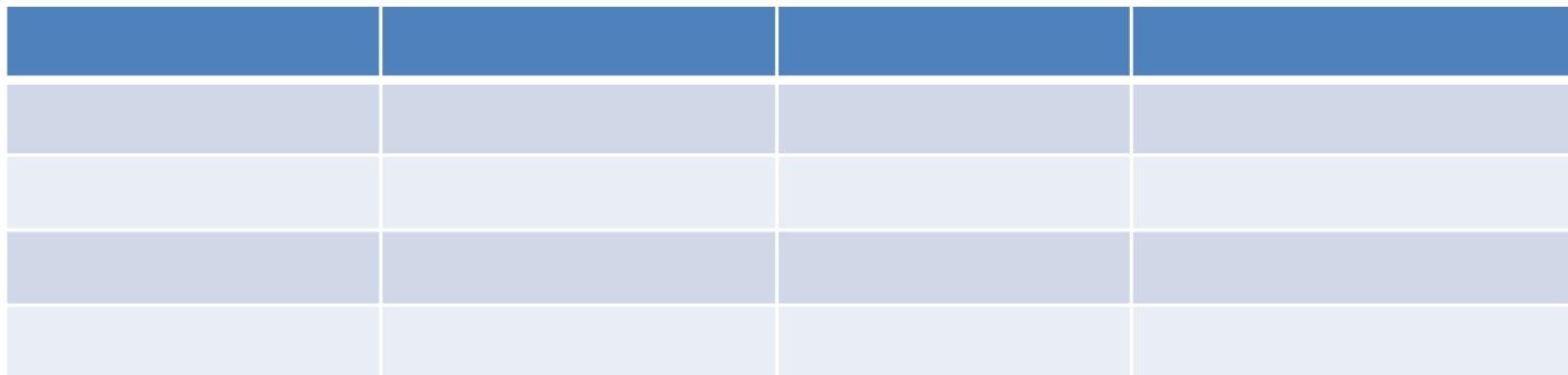
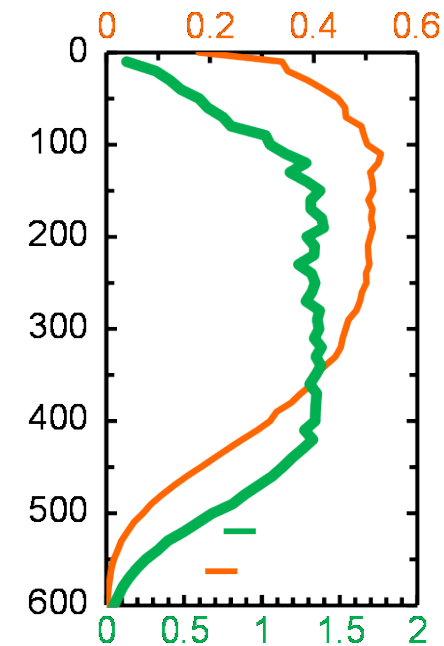
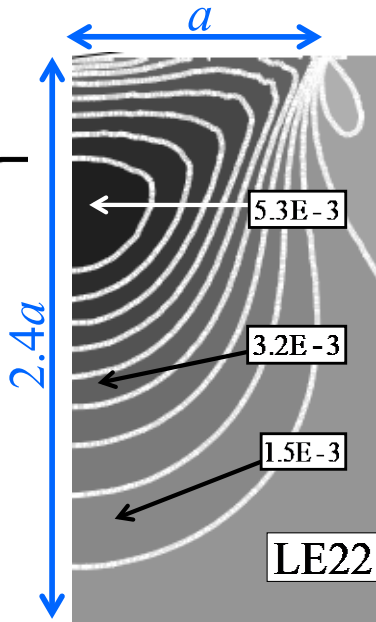
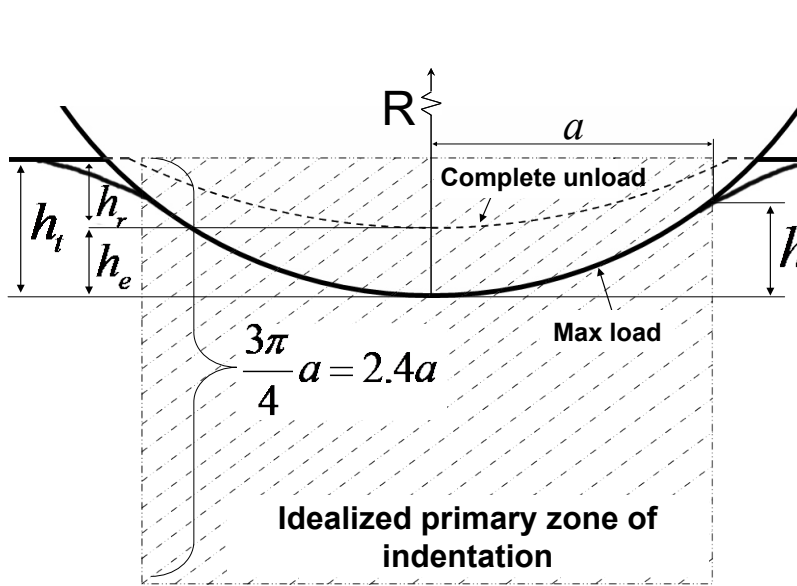
30% deformed Fe-3%Si				
Grain #	Misorientation	Estimated Y_{ind} in the annealed condition, GPa	Measured Y_{ind} in the deformed condition, GPa	% change in τ_{CRSS}
1	7° from (111)	1.12	1.31±0.13	16.9%
2	14° from (001)	0.90	1.07±0.05	18.9%
80% deformed Fe-3%Si				
Region #	Misorientation	Estimated Y_{ind} in the annealed condition, GPa	Measured Y_{ind} in the deformed condition, GPa	% change in τ_{CRSS}
1	20° from (111)	1.12	1.69±0.06	50.9%
2	30° from (001)	1.00	1.46±0.07	46.0%
4	25° from (001)	0.92	1.37±0.07	48.9%
3	10° from (001)	0.85	1.27±0.08	49.4%



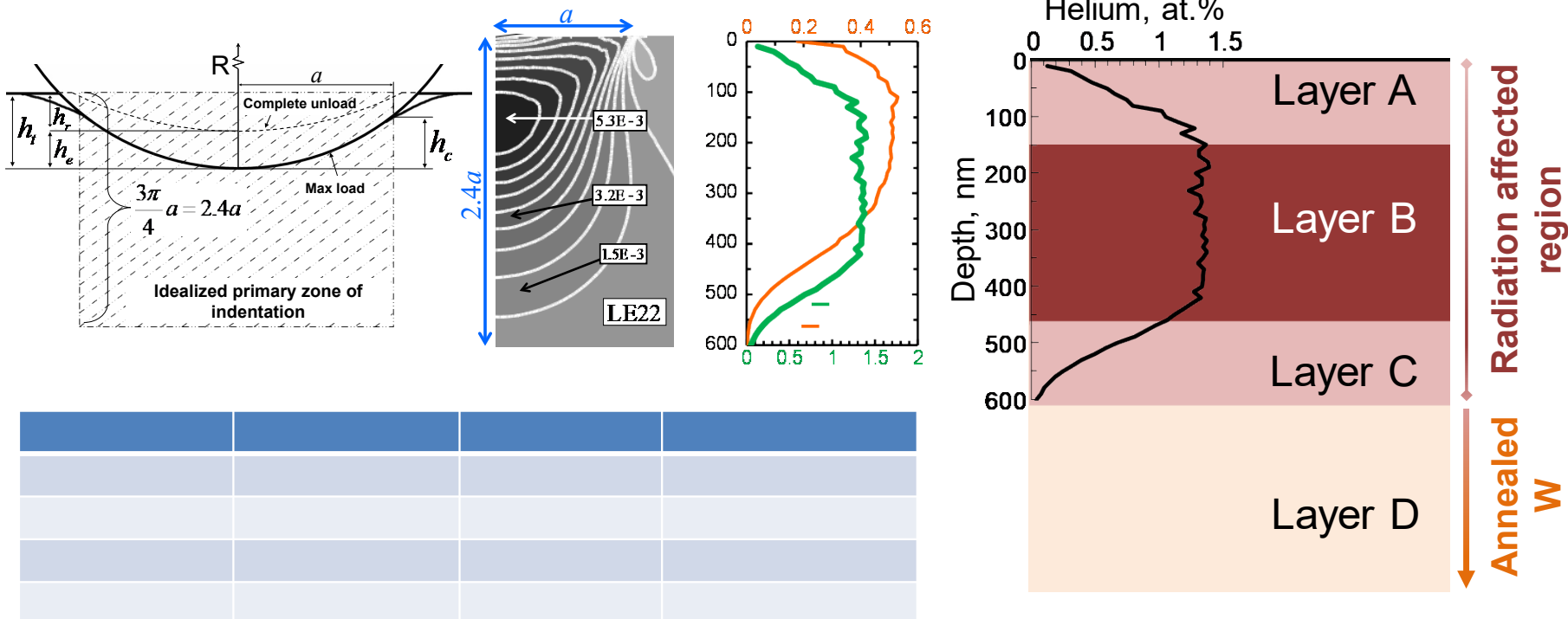
Outline

- Extraction of Spherical Nanoindentation Stress Strain curves
- Indentation on anisotropic samples
- Mechanical response of near grain boundary regions
- Probing nanoscale damage gradients with spherical nanoindentation
- Comparing small scale mechanical test techniques for measuring irradiation hardening

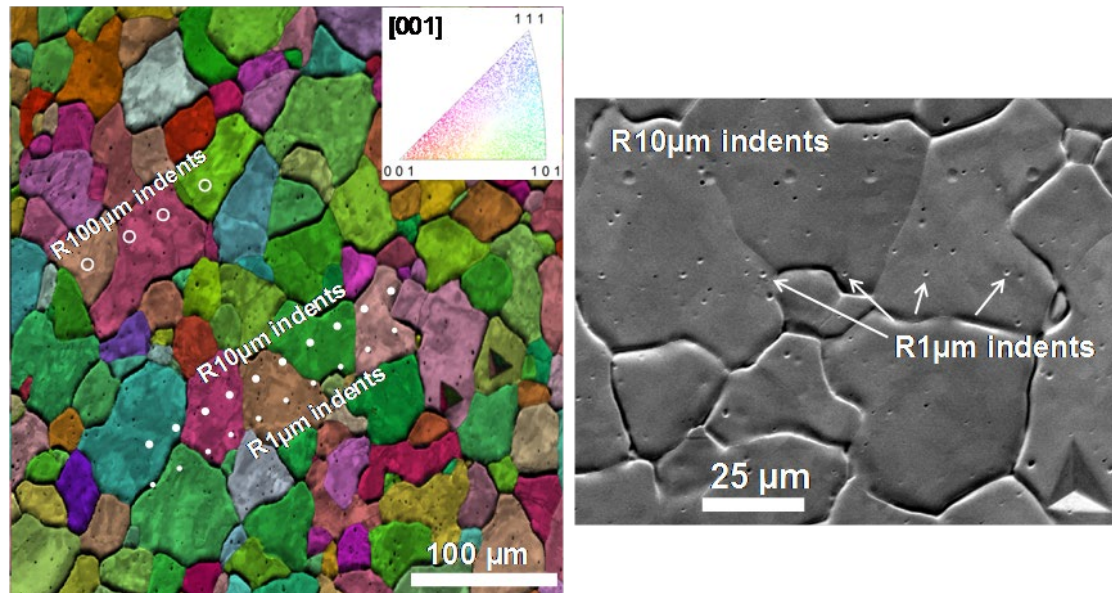
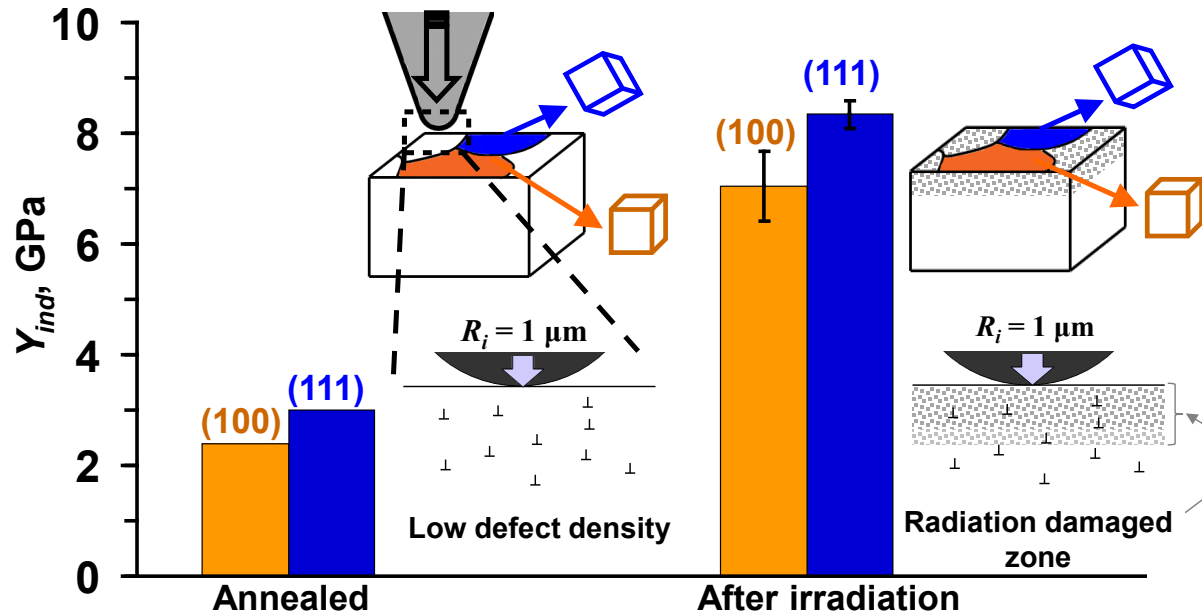
Radiation depth vs. indentation zone



Radiation depth vs. Indentation zone

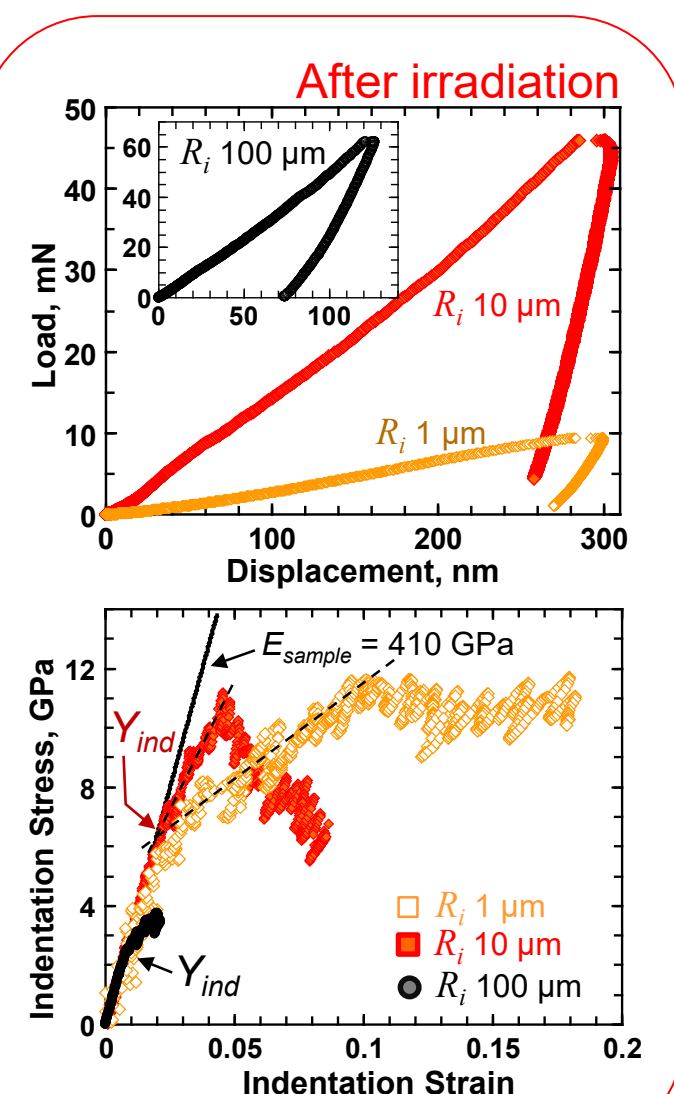
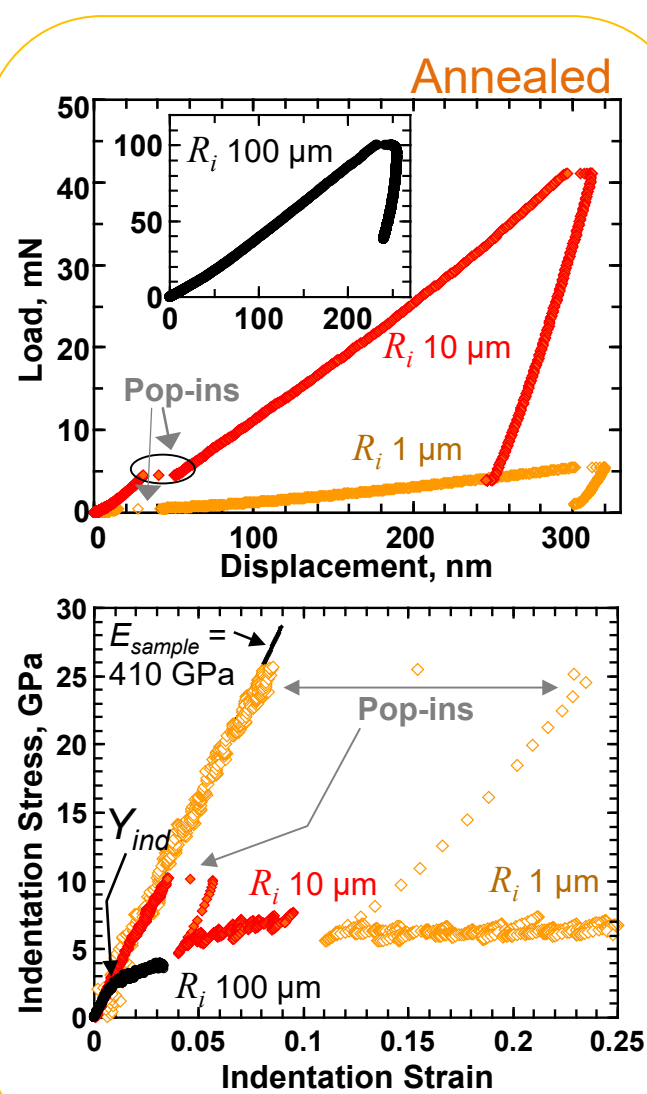


Effect of grain orientation – He on W



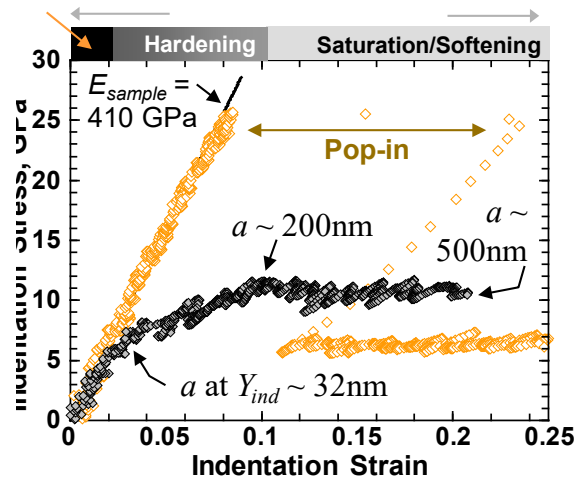
Effect of indenter size, pop-ins disappear after irradiation

Load -
Displacement
[100] oriented

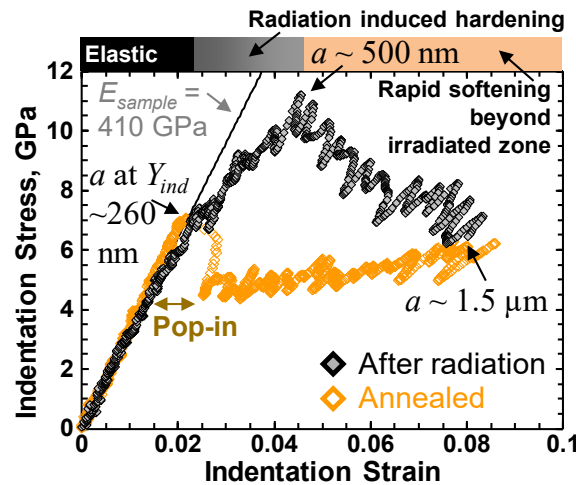


Annealed vs. He irradiated W with varying indenter sizes

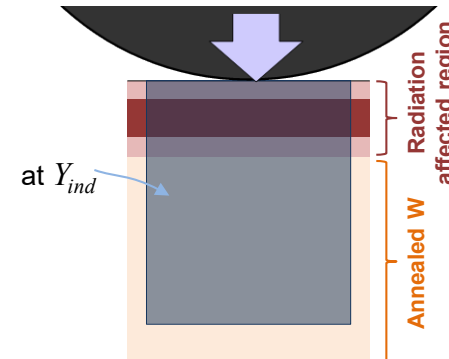
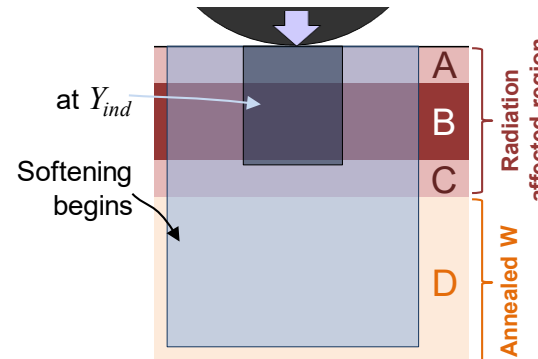
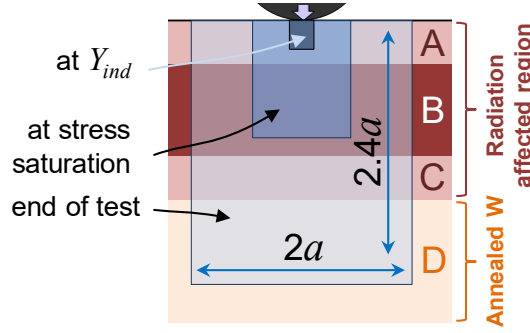
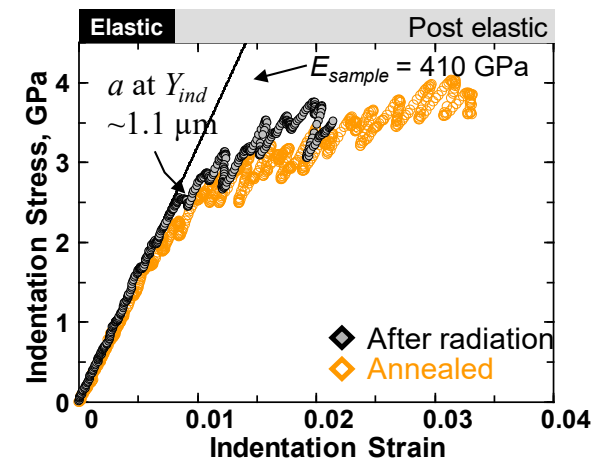
$R_i = 1 \mu\text{m}$



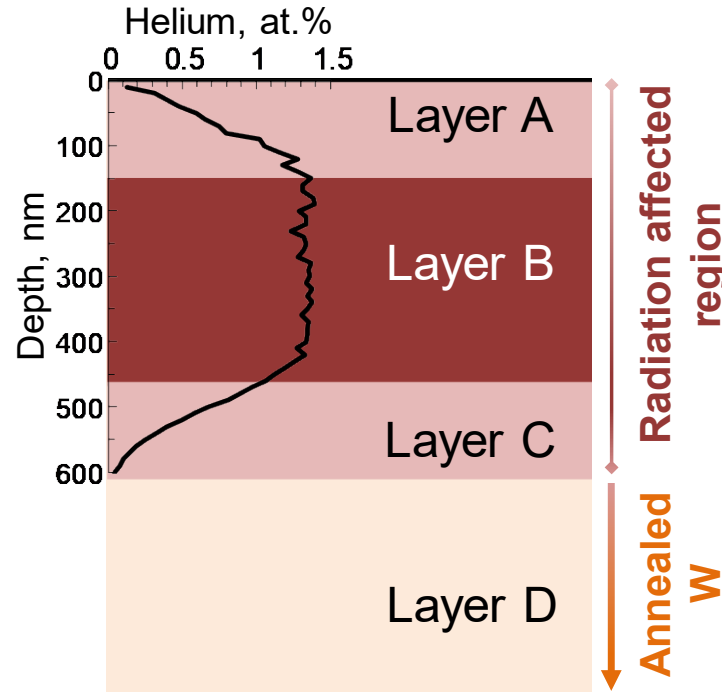
$R_i = 10 \mu\text{m}$



$R_i = 100 \mu\text{m}$

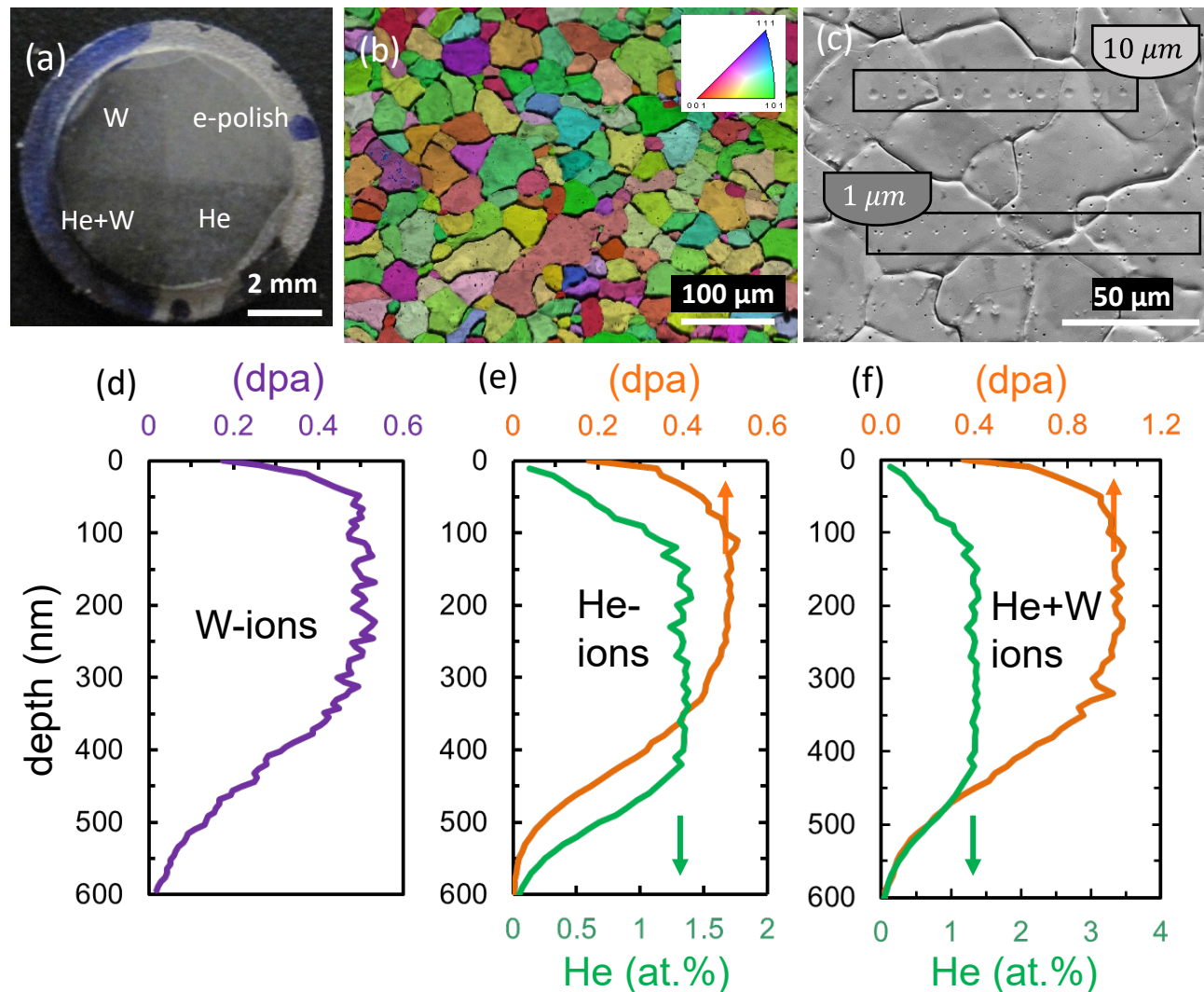


Orientation effect in He irradiated W

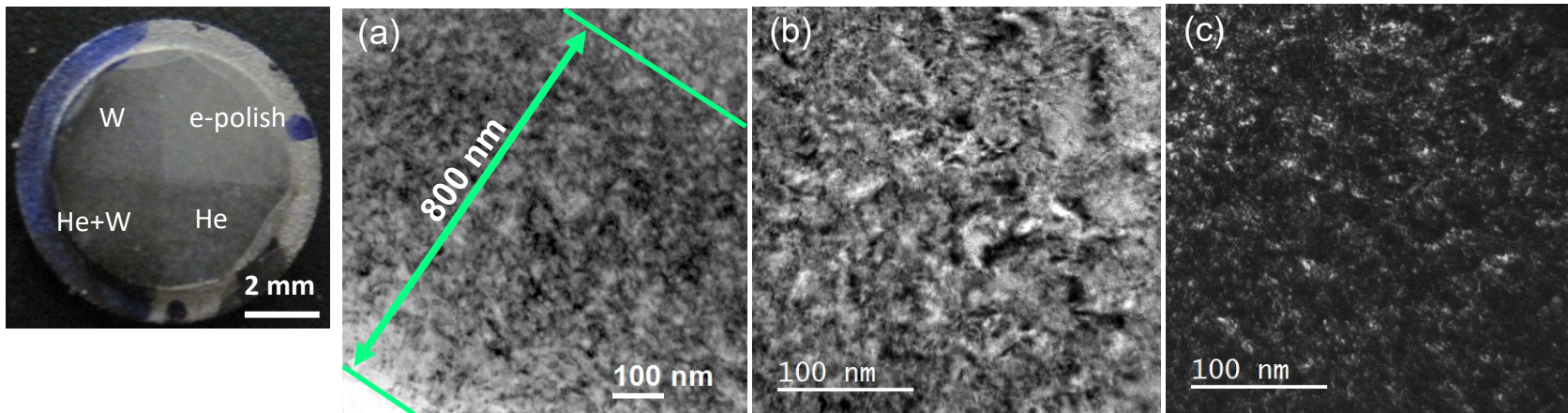


Grain orientation	Layer A Yield stress, GPa	Layer B Yield stress, GPa	Layer D Yield stress, GPa
	Measured as Y_{ind} from $R_i=1 \mu\text{m}$ indenter	Measured as the saturation stress values from $R_i=1, \mu\text{m}$ indenter	Measured as Y_{ind} on annealed W using $R_i=100 \mu\text{m}$ indenter
Near (100)	3.7 ± 0.8	10.1 ± 0.9	2.4 ± 0.4
Near (111)	4.6 ± 0.4	11.3 ± 0.4	3.1 ± 0.3

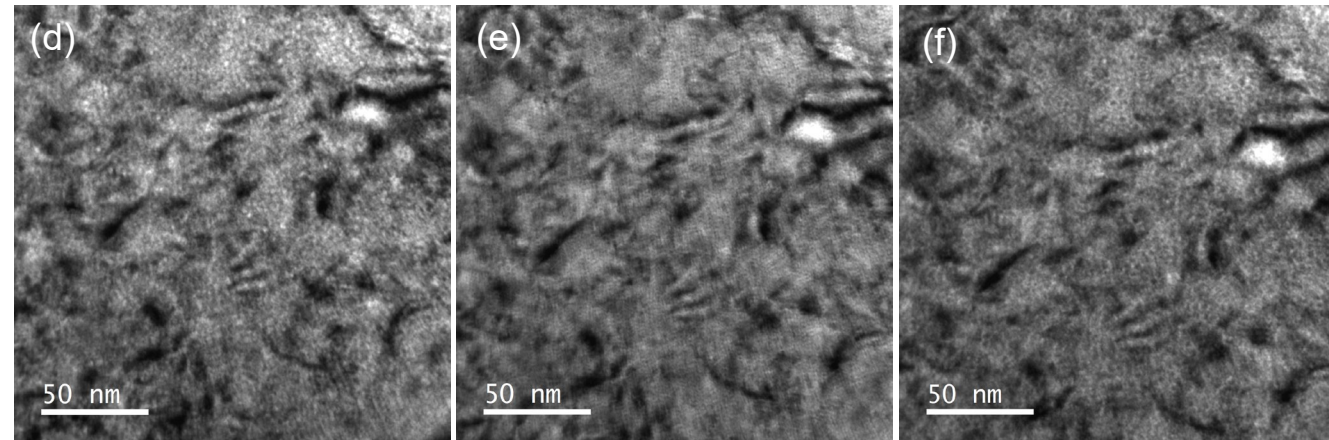
Comparing He, W and He + W ion irradiation on tungsten



Microstructure of He+W ion irradiation on tungsten

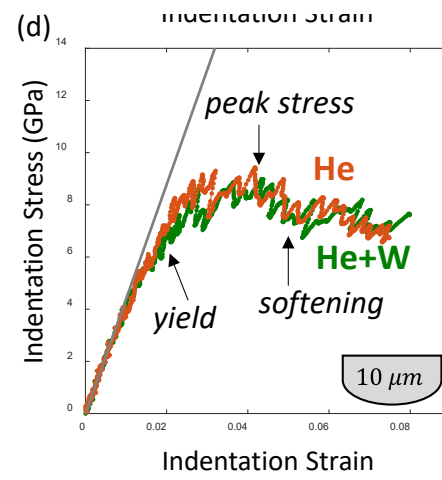
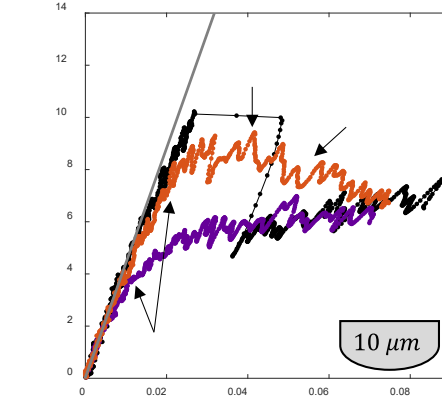
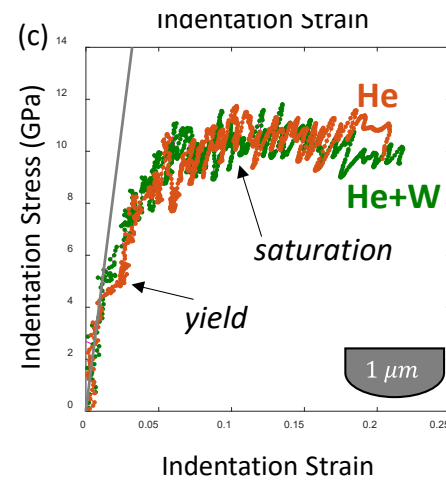
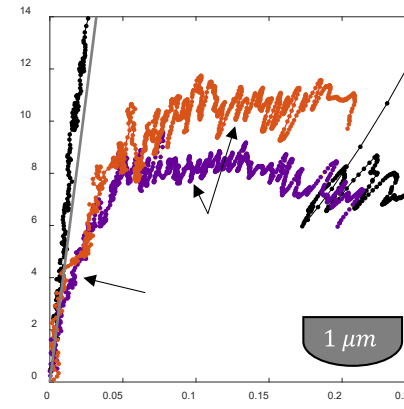
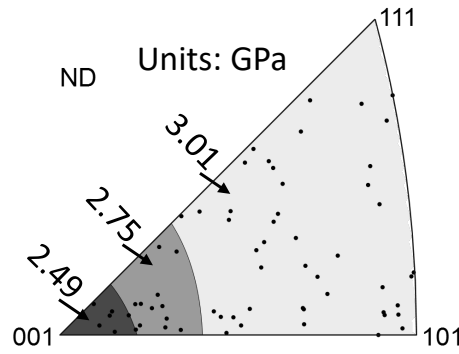
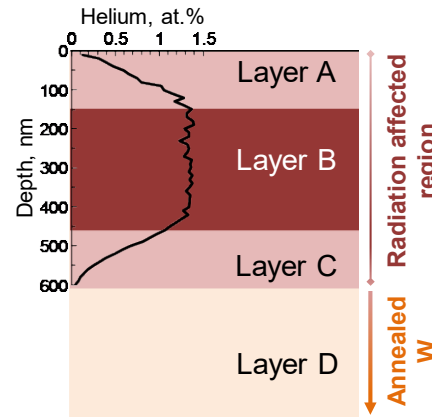


Representative TEM micrographs of the dislocation loops and He bubbles in the irradiated layer for the **He+W** region



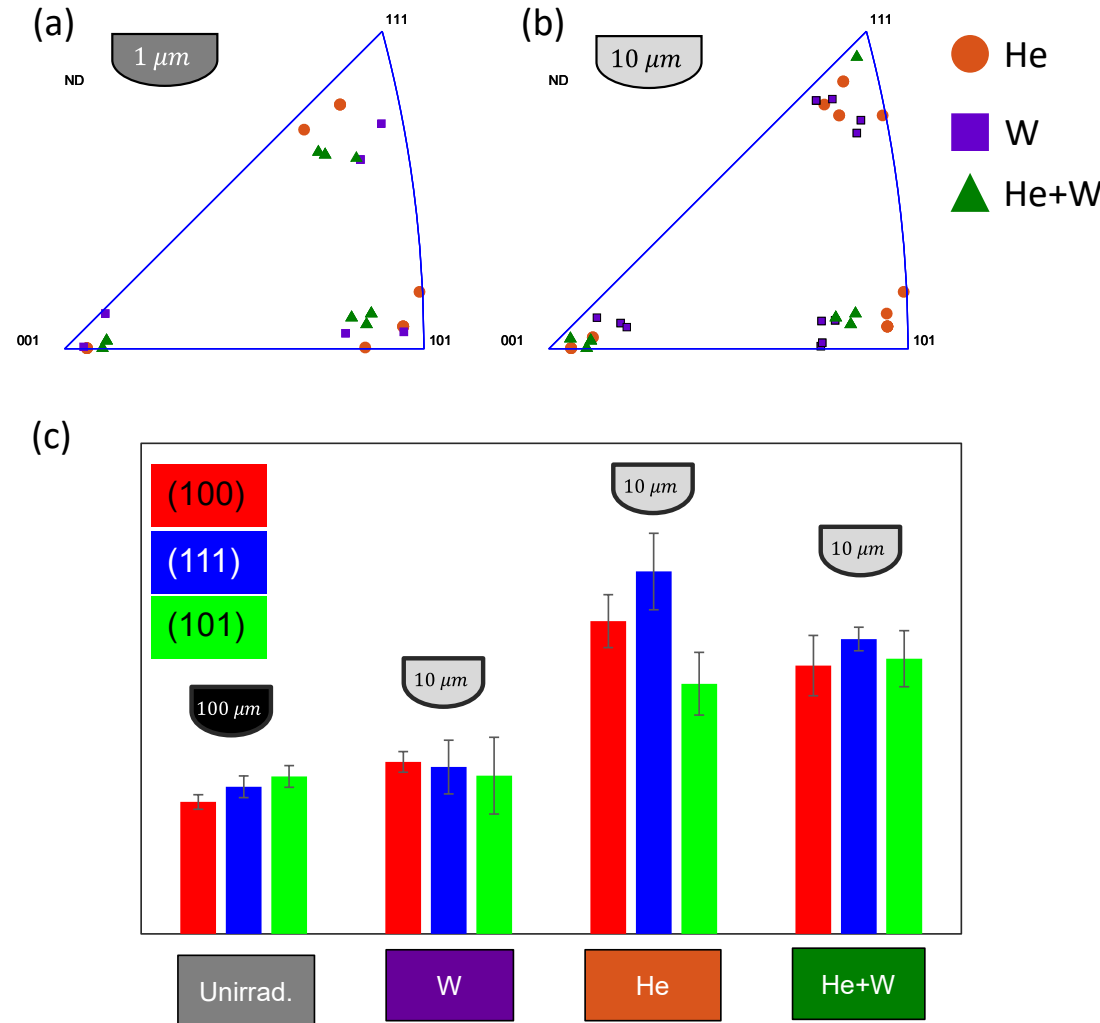
(d-f) under focused, in-focus, and over focused images showing He bubbles.
He bubbles end at a depth of ~ 500 nm

Spherical indentation stress-strain analysis of He, W and He+W ion irradiation on tungsten



- He implanted tungsten exhibits higher plastic flow strengths compared to W irradiated tungsten,
- there is no significant difference between the indentation response of the He and He+W regions despite twice the dpa damage for the He+W compared to the He region,
- the 1 μm indenter response is very similar for all irradiated conditions up to ~5% indentation strain,
- 1 and 10 μm indenters show different responses for the same irradiated material

Effect of crystal orientation on the mechanical response of the irradiated material

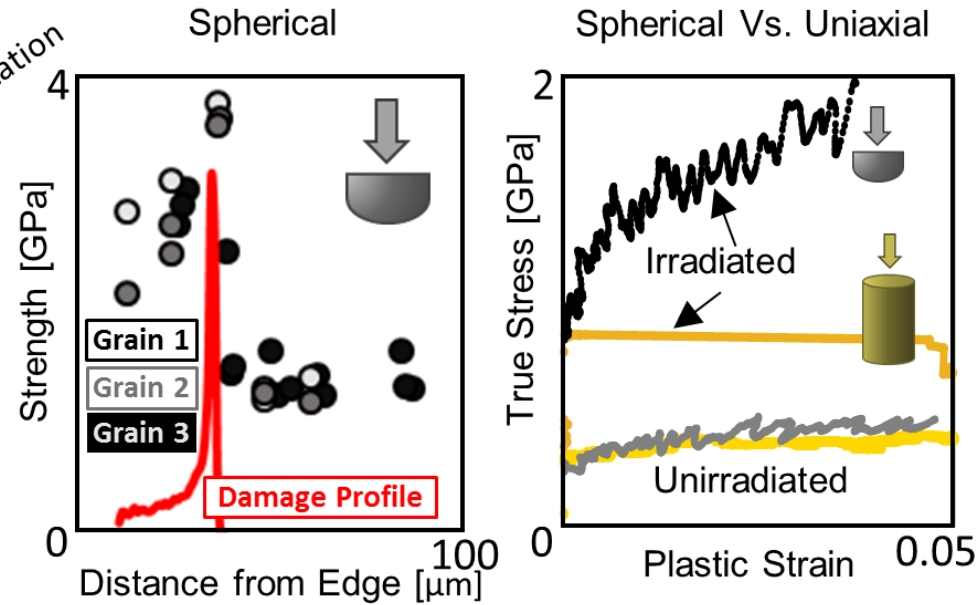
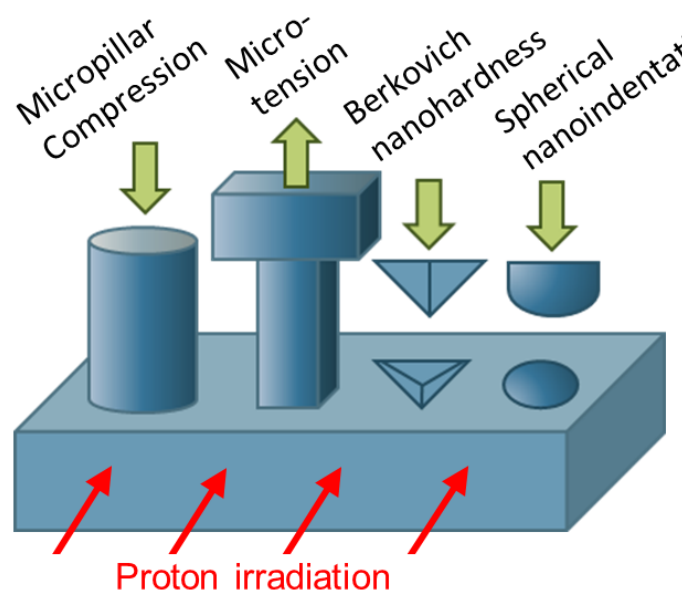


The orientation trend for the indentation yield strength ($Y_{ind}^{(100)} < Y_{ind}^{(111)} \cong Y_{ind}^{(101)}$) present in the unirradiated material is no longer apparent in the irradiated material

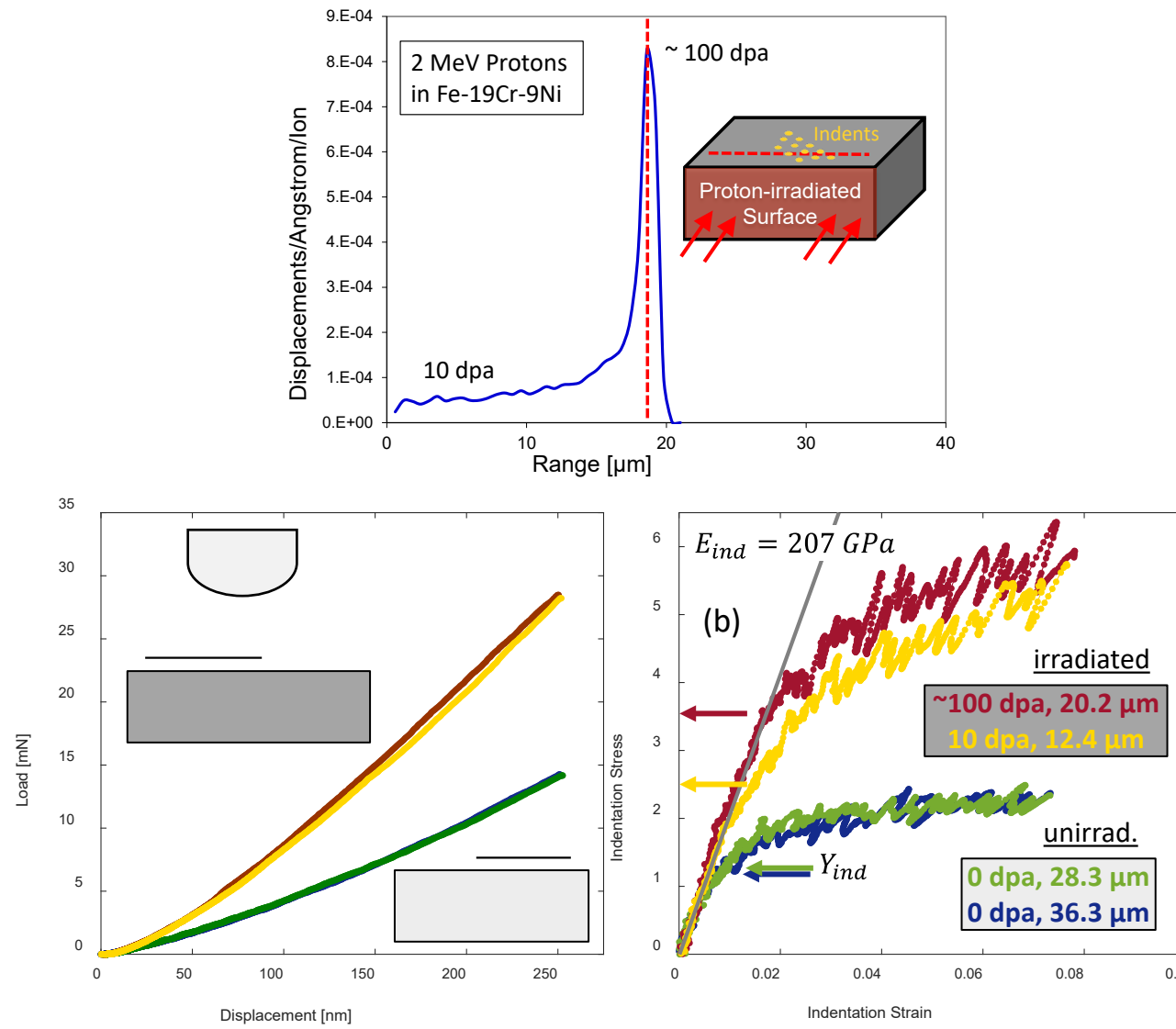
Outline

- Extraction of Spherical Nanoindentation Stress Strain curves
- Indentation on anisotropic samples
- Probing nanoscale damage gradients with spherical nanoindentation
- Comparing small scale mechanical test techniques for measuring irradiation hardening

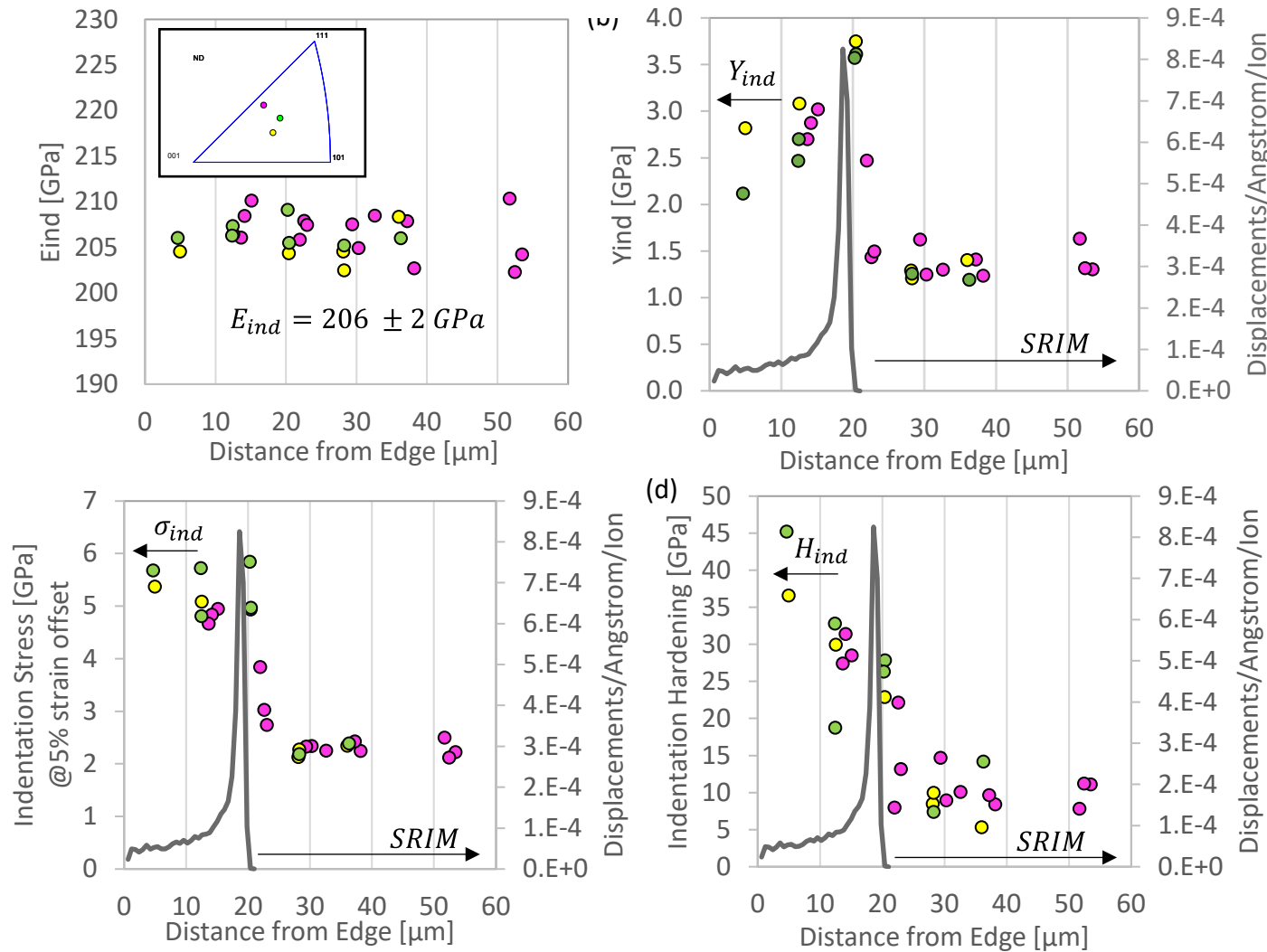
Proton irradiated 304 stainless steel: A comparison of small scale mechanical test techniques for measuring irradiation hardening



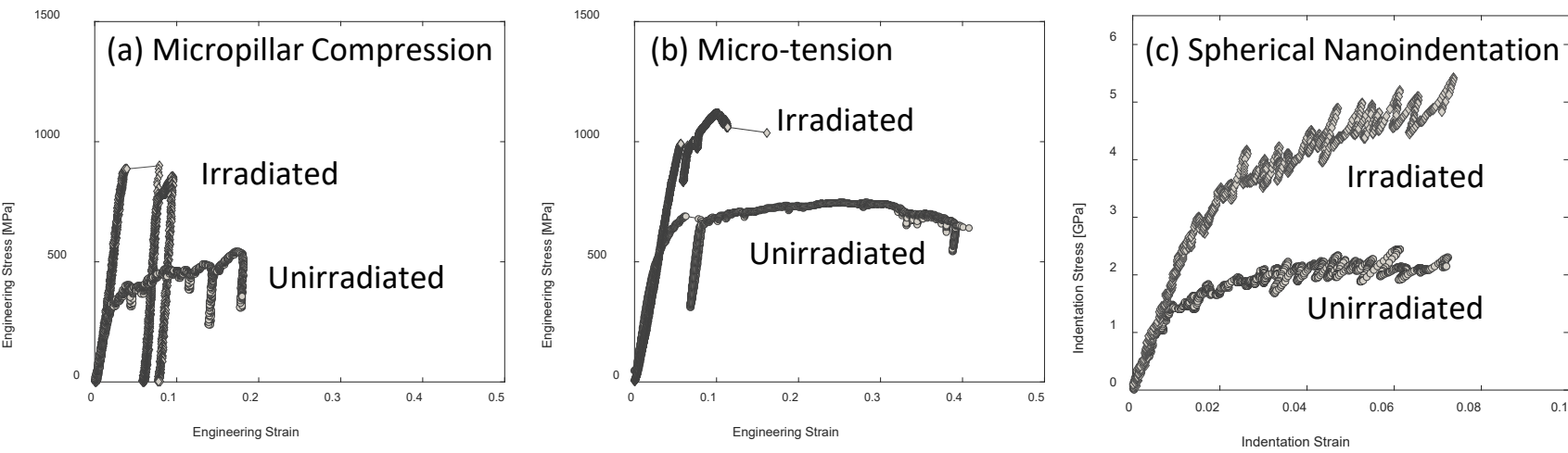
Proton irradiation of 304 stainless steel



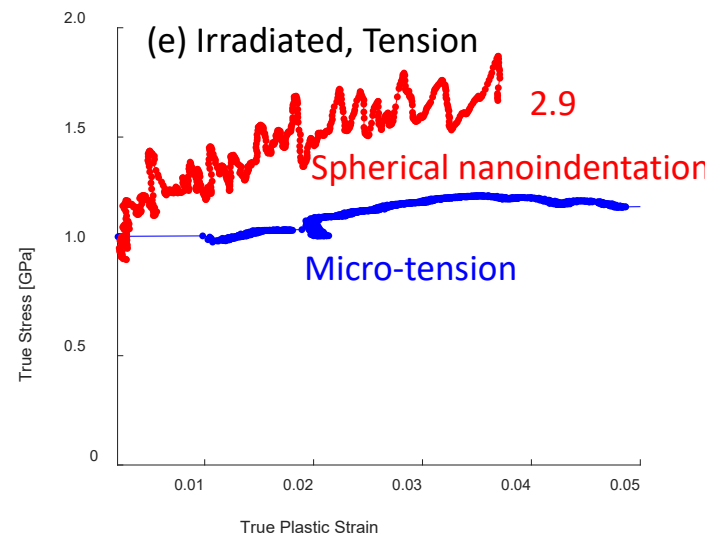
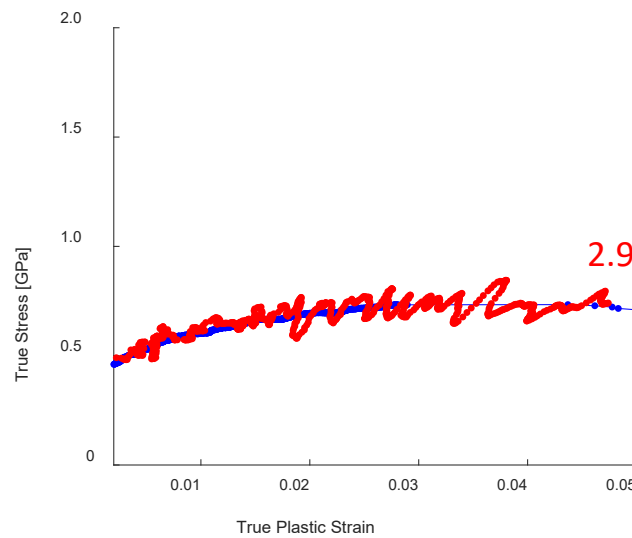
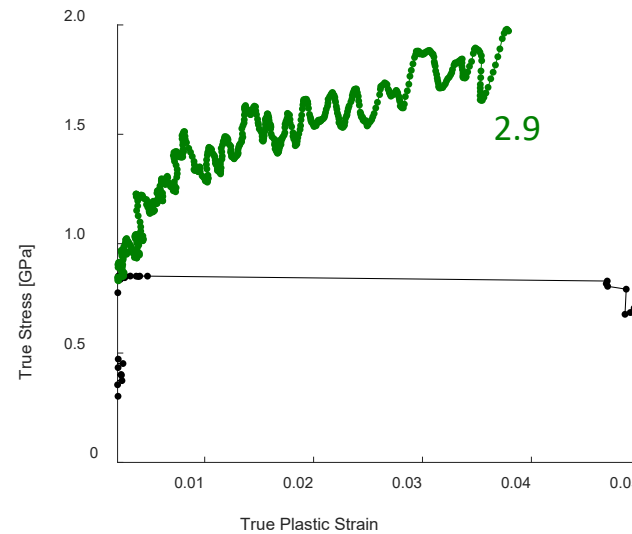
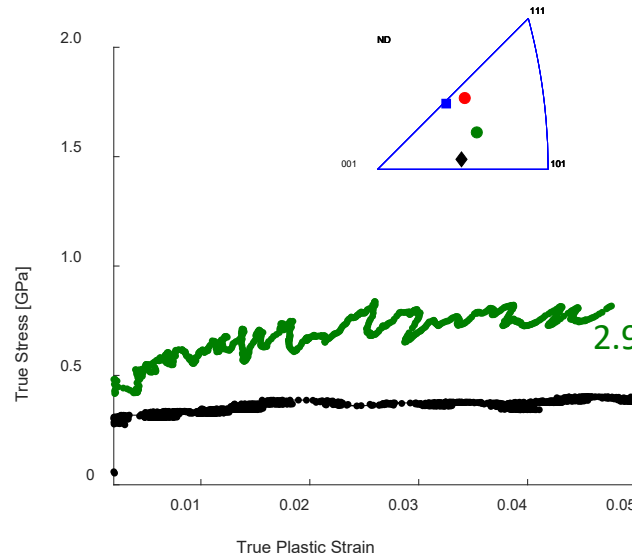
Trends in indentation properties as a function in distance from the edge of the sample



Comparing micro-pillar, micro-tension and spherical indentation

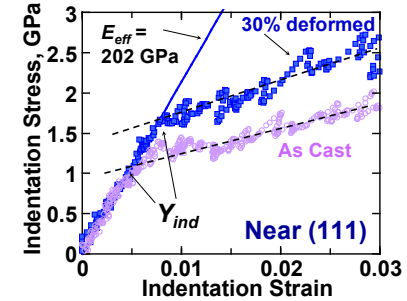


Comparing micro-pillar, micro-tension and spherical indentation

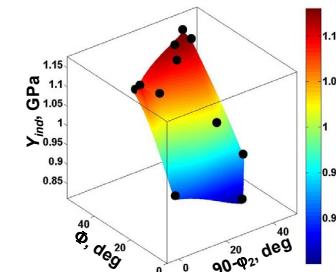


Summary: indentation stress-strain curves

- Indentation stress-strain curves allow us to explore the elastic, yield and post-elastic behavior in a variety of material systems.



- In anisotropic polycrystalline metal samples (Fe-3%Si steel)
 - to characterize the anisotropy (β) in the elastic indentation modulus, and
 - the increase in the indentation yield strength in deformed microstructures



- This technique is now being explored to
 - probe near-interface regions
 - probe the changes in indentation yield strength in ion-irradiated samples

